(This is a sample cover image for this issue. The actual cover is not yet available at this time.)

Journal of African Earth Sciences 63 (2012) 48–61

Contents lists available at SciVerse ScienceDirect

Journal of African Earth Sciences

journal homepage: www.elsevier.com/locate/jafrearsci

Gem-quality Turkish purple jade: Geological and mineralogical characteristics

Murat Hatipoğlu [a,b,*], Yasemin Başevirgen [b], Steven C. Chamberlain [c]

[a] Dokuz Eylül University, İMYO, İzmir Multidisciplinary Vocational School, Gemmology and Jewellery Programme, 35380 Buca-Izmir, Turkey
[b] Dokuz Eylül University, The Graduate School of Natural and Applied Sciences, Department of Natural Building Stones and Gem Stones, 35370 Buca-Izmir, Turkey
[c] New York State Museum, Center for Mineralogy, Albany, NY 12230, USA

ARTICLE INFO

Article history:
Received 26 August 2011
Received in revised form 27 October 2011
Accepted 1 November 2011
Available online 16 November 2011

Keywords:
Purple jade
Confocal dispersive Micro-Raman spectroscopy (DCμRS)
XRF and ICP-AES
XRD
Specific gravity (SG)
Polarized-light microscopy

ABSTRACT

In the Harmancık–Bursa region of the western Anatolia (Turkey), an extensive contact metamorphic aureole at the border between the Late Mesozoic coherent metaclastic rocks of blueschist facies and the Early Senozoic intrusive granodiorite stock hosts an interesting and unique gem material with a mineral assemblage consisting mainly of jadeite, quartz, orthoclase, epidote, chloritoid, and phlogopite as identified by X-ray diffraction spectroscopy and polarized-light microscopy. In addition, chemical analyses performed with X-ray fluorescence and inductive-coupled plasma-atomic emission spectroscopy show that the mass of the metamorphic aureole has a silica-rich, calc-alkaline chemical content. Therefore, some rock building elements (such as Al, Ca, Na, K, P, Sr, and B of which characterize an acidic–neutral rock formation) and trace elements (such as Fe, Cr, Mn, Be, Cu, Ga, La, Ni, Pb, and Zn) are remarkable high ratios.

Pale purple-colored gem material of this composition appears to be unique to Turkey, also is only found in one narrow provenance in Turkey. Therefore, it is specially called "Turkish (and/or Anatolian) purple jade" on the worldwide gem market. Even though the mineral jadeite is the principal constituent, 40% by volume as determined with petrographic thin-section examination under a polarized-light microscope, the material cannot be considered pure jadeite.

Specific gravity measurements of the jade using a hydrostatic balance confirm that it has a heterogeneous structure. The measured average specific gravity of 3.04, is significantly lower than the normal range for characterized jadeites of 3.24–3.43.

Turkish purple jade samples were examined in detail using dispersive confocal micro-Raman spectroscopy (DCμRS) as well as other well-known analytical methods. The resulting strong micro-Raman bands that peaked at 1038, 984, 697, 571, 521, 464, 430, 372, 326, 307, 264, and 201 cm^{-1} are characteristics of the Turkish purple jade. The first most intensive and widest Raman band that peaked at 697 cm^{-1} can be interpreted as the v_2 doubly symmetric bending mode of (SiO_4/M) centers. The "M" includes the some cationic substitutions of Si by Fe, Cr, Mn, Be, Cu, Ni, Pb, and Zn, and also K and Na. The second most intensive and widest Raman band that peaked at 372 cm^{-1} can be interpreted as the v_2 single symmetric bending mode of (SiO_4/M) centers. The third most intensive and widest Raman band that peaked at 201 cm^{-1} can be interpreted as translational libration. Finally, the fourth distinctive Raman bands that peaked at 1038 and 984 cm^{-1} can be interpreted as the v_1 doubly symmetric stretching modes of (SiO_4/M) centers. In addition, both sides of these bands were also barricaded with relatively unimportant Raman bands produced by some structural imperfections.

The measurements of these all analytical parameters are the most trustworthy method to distinguish the purple jade from the other well-known kinds of natural, synthetic, and/or color-enhanced jades. Finally, these parameters provide positive identification of the provenance (geographic origin) of the original Turkish purple jade. The data obtained in this study for dispersive confocal micro-Raman bands, specific gravity values, and trace element contents provide a unique fingerprint for this kind of jadeite-jade gem material.

1. Introduction

The jade as a material is known in many fine nuances of green, but also in shades of white, black, gray, yellow, and orange, and in delicate violet tones. Moreover, all kinds of natural gem-quality

* Corresponding author at: Dokuz Eylül University, İMYO, İzmir Multidisciplinary Vocational School, Gemmology and Jewellery Programme, 35380 Buca-Izmir, Turkey. Tel.: +90 232 3012564.
E-mail address: murat.hatipoglu@deu.edu.tr (M. Hatipoğlu).

1464-343X/$ - see front matter © 2011 Elsevier Ltd. All rights reserved.
doi:10.1016/j.jafrearsci.2011.11.004

jades, either jadeite-jade or nephrite-jade, are extremely rare and highly valued (Harlow and Sorensen, 2005; Harlow et al., 2007). The word "jade" is derived from the Spanish term 'piedra de ijada'. Since, when the Spanish conquered Mexico, they saw that people in Mexico powdered jadeite and sometimes mixed it with water for making a cure against numerous internal diseases. The first recorded use of this term is by Nicol Monardes in a work on medicinal plants of the New World written in 1565 (Crowhurst, 2001; Easby, 1991). The term "jade" as used in the gem trade, in fact, refers to these two minerals: jadeite (pyroxene group) ($Na(Al,Fe)Si_2O_6$) and nephrite (amphibole group) [$Ca_2(Mg,Fe)_5Si_8O_{22}(OH)_2$] (Prewitt and Burnham, 1966; Morimoto, 1988, 1989; Cameron and Papike, 1981; Htein and Naing, 1994). However, jadeite is different in chemical composition from nephrite, and can exhibit highly saturated colors and a higher degree of translucency, a higher hardness, and a glassy appearance (Harder, 1995). Because of its superior features, jadeite quickly replaced nephrite as the "jade" of choice among art and gem collectors. Contemporary descriptions of "imperial" jadeite cite the following qualitative attributes; a very intense and uniform green color ranging from "apple green" to "spinach green"; a high degree of uniform translucency; and an extremely smooth finish with a greasy feel and lustre (Nassau and Shigley, 1987; Zhao et al., 1994; Nestola et al., 2007; Bersani and Lottici, 2010).

Before the 18th century, only nephrites had been found, mined, and carved into art objects or jewellery. During the 1700's, green and/or white colored jadeites were found worldwide localities. Instead of nephrite, jadeite is closely associated with two ancient civilizations, those of Mesoamerica (Mexico, Guatemala, and Belize) and China. Therefore, jadeite material was also used by most of the major civilizations in ancient Mesoamerica; the Olmec, Aztec, Maya, and so forth. Also, this gem, "royal gem" in China, was used in prehistoric times as an ideal tough material for weapons and tools (Andrews, 1986; Easby, 1991; Middleton and Freestone, 1995; Smith and Gendron, 1997).

The cut and polished jadeites as loose stones and/or mounted stones on historic and archeological artifacts have been extracted from the various archeological excavations in Europe and Turkey so far. However, the reported being in existence of the rough green jadeite occurrences (deposits) in Europe and Turkey are very rare. The Western Alps and Austria in Europe appear to be the main source of jadeite mineral and jadeite-jade material (with including the some other minerals) (Bishop et al., 1977; Biino and Compagnoni, 1992; Adamo et al., 2006; Crowhurst, 2001; Harlow et al.,

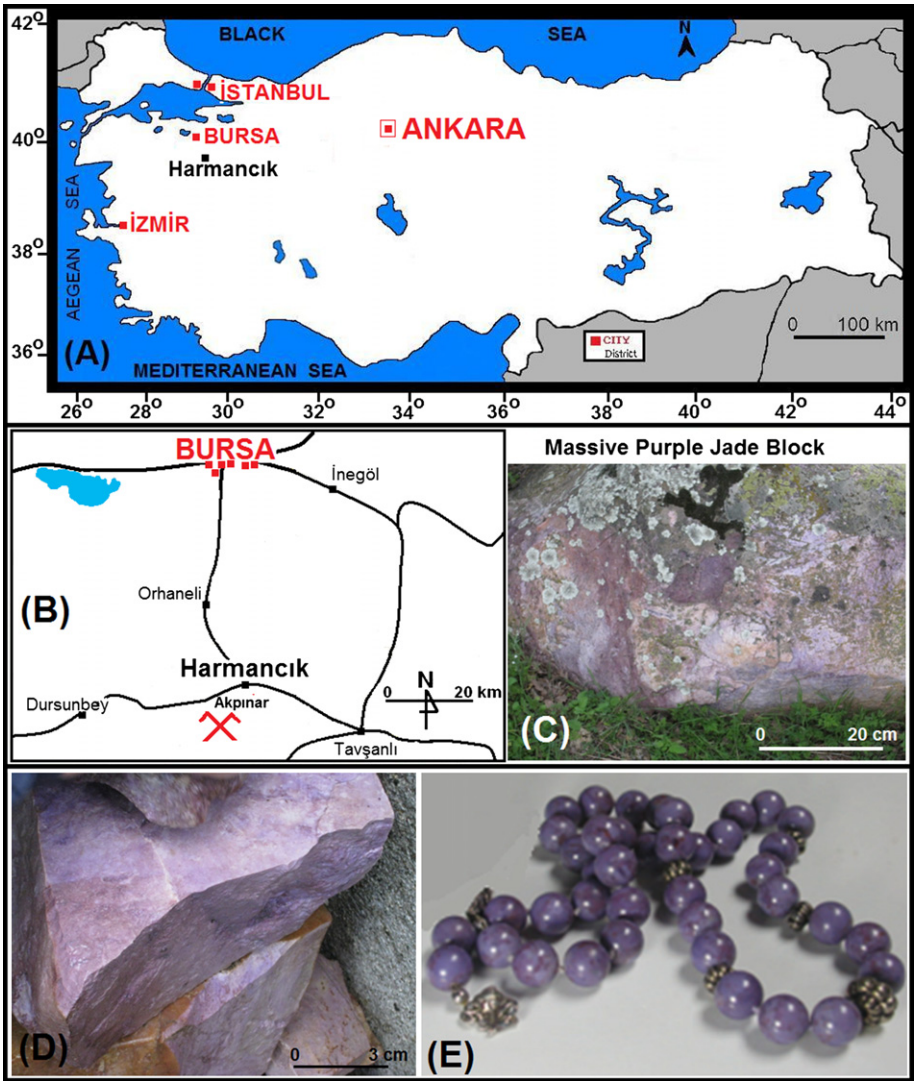

Fig. 1. Location maps showing the Harmancık–Bursa region in Turkey (A) and (B). The fine-grained Turkish purple jade material is found as giant blocks in the field (C). Large-broken fragments of gem-quality purple jade rough are the most valuable on the worldwide gem market (D). Cut and polished gem objects such as these jade and silver prayer beads are widely used in Turkey (E).

2007; Teixeira et al., 2010). However, instead of lavender jadeite, purple colored jade material has been found in a one location in Turkey during the 1970s (Fig. 1A and B). Preliminary and then detailed investigations of the geological studies comprising the Harmancık–Bursa region reveal that these massive material mass (Fig. 1C) belongs to a metamorphic zone in the border between a Late Mesozoic aged coherent blueschist metamorphic sequence and an Early Senozoic aged intrusive granodiorite (Okay, 1980, 1984, 1997, 2002; Okay and Kelley, 1994; Okay et al., 1998). Also, preliminary features of this kind of jade were reported (Digennaro et al., 1997). Some tons of the material have been commercially exploited, and exported with a specific name as "Turkish and/or Anatolian purple jade" since the 1980s. Therefore, the many polished purple jade gem objects and also rough gemstone specimens (Fig. 1D and E) have already been preserved in museums and private collections around the world, that their origin is acknowledged to be only the deposit in the Harmancık–Bursa region of Turkey (Hatipoglu, 2010; Tuncer-Arslanlar et al., 2011).

Since FT-Raman and/or Dispersive (Vis)-Raman vibrational bands were first discovered in the 1920s (Raman and Krishnan, 1928). Raman spectrometers have attracted attention in industrial and academical researches. The micro-Raman spectroscopy is a non-destructive and non-invasive investigation technique in principles of high speed and accuracy. In addition, it can be also used for finite-precision analysis in combination with microscopy (Gouadec and Colomban, 2007; Colomban and Prinsloo, 2009; Fan et al., 2009). The frequency wave number of the Raman scattering signal is a reflection of the vibration and rotational modes of the molecule (Lewis and Edwards, 2001; Slodczyk and Colomban, 2010; Vandenabeele, 2010). Raman maps are images generated from automated recordings of spectra at discrete points of the sample. They show the variation of any fitted parameter (i.e. intensity, width or position of one band) as a function of the point of analysis. If the mapping is regular and sufficiently tight, one gets a "smart map" of the parameter (color or contrast scaling) superimposed with the optical image of the probed area. Raman mapping is not to be mistaken for direct Raman imaging where a large area of the sample is probed all at once and no fitting is required. More precisely, only photons from a narrow spectral domain are sent to the CCD mosaic and each pixel receives those coming from a given area of the sample. The intensity of the signal, thus, reveals the presence and location of any substance with a strong Raman signal in the selected spectral window (Gouadec and Colomban, 2007; Colomban and Prinsloo, 2009). Hanni et al. (1997) reported some important studies on the gemmological applications of Raman spectroscopy. They showed that the Raman systems used so far were working with a microscope to analyse the surface or sub-surface of materials in the confocal mode (Hanni et al., 1997). The analytical method, therefore, analysed the host gemstone, mineral inclusions or organic fillers for hiding fissures. In addition, databases with Raman spectra of gemstones have been published by Delé-Dubois et al. (1986) in the literary, and also RRUFF (2011) on the internet.

Consequently, some of the further analytical methods approach with a non-destructive and non-invasive way during the investigation of a gemstone sample by simply focusing the scope objective focal point to different depths in the sample. Therefore, especially micro-Raman spectroscopy was introduced into the gemmology field in the late twenty century. Moreover, it is becoming more and more important in mineral research, and many related applications have been reported by many researchers (Gendron et al., 2002; Bersani and Lottici, 2010; Fan et al., 2009). Thus, it can be proposed that dispersive confocal micro-Raman spectroscopy (DCμRS) is a well-known method for the analyses of gem-minerals. However, DCμRS has not yet been widely used for the purple jade identification and determination.

This study aims: (1) to give geological formation conditions of purple jade gemstone, (2) to establish geographical provenance of the single known mine deposit of purple jade, (3) to indicate trustworthy characterization parameters for these naturally occurring precious Turkish purple jade specimens, including dispersive confocal micro-Raman vibrational bands, X-ray diffraction patterns, specific gravity values, polarized-light microscope images, and major and trace element contents, and thus (4) to permit Turkish purple jade to be able to distinguish from the other natural and synthetic jades, and/or color-enhanced jades.

2. Materials and methods

In this study, the investigated purple jade samples were taken from the region near the village of Akpınar in the district of Harmancık (Bursa-Turkey) (Fig. 1A and B). Even though jades with green and white color deposited in many worldwide localities have been known since ancient times, no location with a large deposit including gem-quality purple jade has been reported in the literature before. Therefore, the world's only known supply of purple jade is found in the region where geologically investigated in this study. The most typical rough blocks (Fig. 1C) of the purple jade material are obtained from the currently unexploited field in the Akpınar area in this region. The massive material (Fig. 1D), fine-grained rather than coarsely crystalline, is very suitable for cutting into various gem objects (Fig. 1E).

The specific gravity (SG) values of the ten purple jade samples were measured using a SG kit and very sensitive electronic balance (measurement sensitivity of 0.001), and were acquired to be based on the formula ($SG = W_{air}/W_{air} - W_{water}$). The test was performed in the DGL-Gemmological Testing Laboratory at Dokuz Eylül University.

The base building components of the purple jade samples were detected using X-ray powder diffraction pattern analysis, using a Cubi-XRD device with a Cu tube and a graphite monochromotor. The representative samples were analyzed with Cu radiation and a 0.3 mm collimator at atmospheric pressure for 10 min each, in the range between 5° and 70° (2-theta). The d-spacing (Å) diffraction matching of the constituent minerals obtained using the comparative matching technique is based on the positions of peaks with relative intensities ($\%(I/I\max) \geqslant 4$], 2-theta values below 70°, and a tolerance range of ±0.01 (Table 1). X-ray powder diffraction patterns were taken in the Research Laboratory of the Batı Anadolu Cement Factory in Izmir (Turkey).

Polarizing microscope images with ×4 (a combined magnification of ×0.4 objective and ×10 ocular), ×10 (a combined magnification of ×1 objective and ×10 ocular) and ×40 (a combined magnification of ×1 objective and ×40 ocular) magnifications under crossed nicols (+N) (active polarizer and analyzer) of the purple jade samples were observed from thin sections using an Olympus BX41 binocular polarizing microscope with a high-intensity 6 V, 30 W halogen light source combined with a U-CPA and U-OPA optical systems in the Microscopy Laboratory of the Department of Geology at Dokuz Eylül University.

Chemical analyses of the purple jade samples were performed using X-ray fluorescence (XRF) for major oxides and inductively-coupled plasma-atomic emission spectroscopy (ICP-AES) for trace elements, as well as WST-SIM to determine ignition losses. These analyses were certified with the code number "IZ10041271 of Izmir/Turkey branch", under contract by the accredited ALS Chemex Laboratory in Canada.

The dispersive confocal micro-Raman spectroscopy of the purple jade samples were performed on a dark background at room temperature using a HORIBA Jobin Yvon Scientific XPLORA dispersive confocal micro-Raman spectrometer (DCμRS) with a high

Table 1
Numerical data obtained from XRD analysis of a representative Turkish purple jade sample.

CUBI-XRD
Sample identification: M0251110
Data measured at: 25-NOV-2010
Tube anode: Cu
Wavelength Alphal (Å): 1.54056
Wavelength Alpha2 (Å): 1.54439
Start angle (°2θ): 5.015
End angle (°2θ): 70.025
Maximum intensity: 7551.610
Intensities converted to: FIXED
Number of peaks: 66

Angle (°2θ)	d-value α1 (Å)	d-value α1 (Å)	Peak width (°2θ)	Peak int (counts)	Back. int (counts)	Rel. int (%)	Signif.
8.845	9.9893	10.0141	0.120	2162	331	28.6	5.99
13.890	6.3703	6.3862	0.090	130	174	1.7	1.01
14.235	6.2167	6.2322	0.150	154	1.66	2.0	1.86
17.740	4.9956	5.0080	0.120	557	130	7.4	3.30
19.910	4.4557	4.4668	0.150	346	114	4.6	2.03
20.850	4.2569	4.2675	0.120	1467	108	19.4	7.91
22.635	4.1042	4.1144	0.090	88	104	1.2	0.88
22.935	3.8744	3.8840	0.150	231	98	3.1	2.63
23.855	3.7270	3.7363	0.120	269	94	3.6	1.87
25.525	3.4868	3.4955	0.180	339	86	4.5	5.49
26.640	3.3434	3.3517	0.150	7552	83	100.0	31.85
27.400	3.2523	3.2604	0.090	154	81	2.0	2.00
27.890	3.1963	3.2043	0.180	384	79	5.1	5.73
28.740	3.1037	3.1114	0.210	259	77	1.4	8.83
29.895	2.9863	2.3938	0.180	538	74	7.1	6.68
30.565	2.9224	2.9297	0.180	713	72	9.4	9.17
31.245	2.8603	2.3674	0.180	357	71	4.7	1.45
31.575	2.8312	2.8362	0.150	1584	69	21.0	12.89
32.050	2.7903	2.7972	0.180	246	69	3.3	3.90
32.835	2.7254	2.7321	0.120	56	67	0.7	0.90
33.515	2.6716	2.6782	0.150	28	61	0.4	0.99
34.125	2.6252	2.6313	0.180	61	64	0.8	0.85
34.630	2.5881	2.5945	0.180	166	62	2.2	0.82
35.060	2.5573	2.5637	0.300	376	62	5.0	12.22
36.000	2.4927	2.4989	0.210	310	61	4.1	7.27
36.540	2.4571	2.4632	0.150	562	59	7.4	8.09
37.150	2.4181	2.4241	0.180	321	58	4.3	6.71
37.820	2.3763	2.3827	0.240	106	56	1.1	2.27
39.455	2.2820	2.2877	0.150	372	55	4.9	7.15
40.285	2.2369	2.2424	0.180	240	53	3.2	6.11
40.870	2.2062	2.2117	0.180	199	52	2.6	4.31
41.805	2.1590	2.1644	0.180	104	52	1.4	2.92
42.445	2.1279	2.1332	0.180	475	50	6.3	9.22
43.700	2.0697	2.0748	0.180	222	49	2.9	3.09
44.185	2.0481	2.0531	0.120	132	49	1.8	1.22
45.380	1.9969	2.0018	0.180	445	18	5.9	6.51
45.785	1.9801	1.9851	0.090	266	48	3.5	0.80
46.095	1.9675	1.9724	0.180	180	46	2.4	1.07
46.660	1.9450	1.9499	0.180	50	46	0.7	1.29
48.105	1.8899	1.8946	0.210	31	45	0.4	2.10
49.520	1.8392	1.8437	0.120	41	44	0.5	0.80
50.125	1.8184	1.8229	0.180	630	44	8.3	14.63
51.905	1.7601	1.7645	0.180	169	42	2.2	5.11
52.915	1.7289	1.7332	0.300	66	41	0.9	3.18
54.410	1.6849	1.6891	0.240	71	40	0.9	1.38
54.850	1.6724	1.6765	0.120	231	40	3.1	3.20
55.315	1.6594	1.6635	0.120	166	40	2.2	1.10
55.830	1.6453	1.6494	0.300	159	38	2.1	3.30
56.585	1.6252	1.6292	0.180	79	38	1.0	1.63
57.120	1.6112	1.6152	0.240	71	38	0.9	1.16
57.725	1.5957	1.5997	0.180	48	38	0.6	0.97
58.650	1.5728	1.5767	0.210	166	37	2.2	5.05
59.555	1.5510	1.5549	0.240	161	37	2.1	4.48
59.935	1.5421	1.5459	0.090	462	36	6.1	2.36
60.765	1.5230	1.5268	0.420	96	36	1.3	6.26
61.850	1.4988	1.5026	0.120	222	36	2.9	0.90
62.795	1.4785	1.4822	0.180	64	35	0.8	1.14
63.490	1.4640	1.4677	0.180	69	35	0.9	2.80
64.015	1.4533	1.4569	0.120	114	35	1.5	1.61
65.245	1.4288	1.4324	0.150	56	34	0.7	1.07
65.860	1.4170	1.4205	0.300	37	34	0.5	1.66
67.715	1.3826	1.3860	0.120	279	32	3.7	3.58

(*continued on next page*)

Table 1 (*continued*)

Angle (°2θ)	d-value α1 (Å)	d-value α1 (Å)	Peak width (°2θ)	Peak int (counts)	Back. int (counts)	Rel. int (%)	Signif.
							(*continued pn next page*)
68.110	1.3750	1.3784	0.090	357	32	4.7	1.12

throughput integrated spectrograph. The spectrometer uses one laser excitation of about 532 nm. Spectral characteristics are displayed on spectra. Operating temperature is between 15 and 28 °C. Spectral manipulation as baseline adjustment was carried out using the software of the device. The Raman record was carried out in the DGL-Gemmological Testing Laboratory at Dokuz Eylül University.

3. Results and discussion

3.1. Provenance, geological setting, and mineralogical implications

In this study, the geology of the region around the deposit of purple jade was re-investigated, taking into account previous field observations. The resulting, simplified geological map and cross-section of the area around the village of Akpınar in the Harmancık–Bursa region (Turkey) are shown in Fig. 2, which is interpreted and modified from Kaya et al. (1989) and Okay (1997, 2002).

During the geological field investigation, it was noted that the Harmancık–Bursa region displays, in large scale, the complex geological formations belonging to two different continental crusts (the Sakarya Continent to the north and the Anatolide–Toride Block to the east) separated by the Tethyan Ocean during the Mesozoic Period. By the beginning of the Tertiary, these two terrestrial blocks had collided, and the region was tectonically affected by the Late Alpine Orogenesis (Sengör and Yilmaz, 1981; Bingöl et al., 1982; Kaya et al., 1989; Yilmaz et al., 2010).

In this study, the coherent rocks units called the Tavşanlı Zone are of particular interest, since these rock units contain the purple jade material that is the main interest of this paper. The Tavşanlı Zone constitutes one of the largest and best preserved glaucophane-lawsonite blueschist belts in the world. The Cretaceous blueschist became tectonically overlain by a Cretaceous oceanic accretionary complex and ophiolite. The suture separating the two zones is represented by a major strike-slip fault (Okay, 1980, 1984, 1997, 2002; Okay and Kelley, 1994; Okay et al., 1998). Accordingly, the region lying from the north-western (Orhaneli-Bursa) to the south-eastern (Tavşanlı-Kütahya) is mainly covered with a blueschist metamorphic complex sequence that is south of the main Neo-Tethyan suture (Kaya et al., 1989; Okay et al., 1998). Overall, the region represents a subducted former continental crust now present as a blueschist terrain in the orogenic belt.

However, in order to simplify, all geological units can be collected under three main groups: (1) blueschist metaclastic rocks;

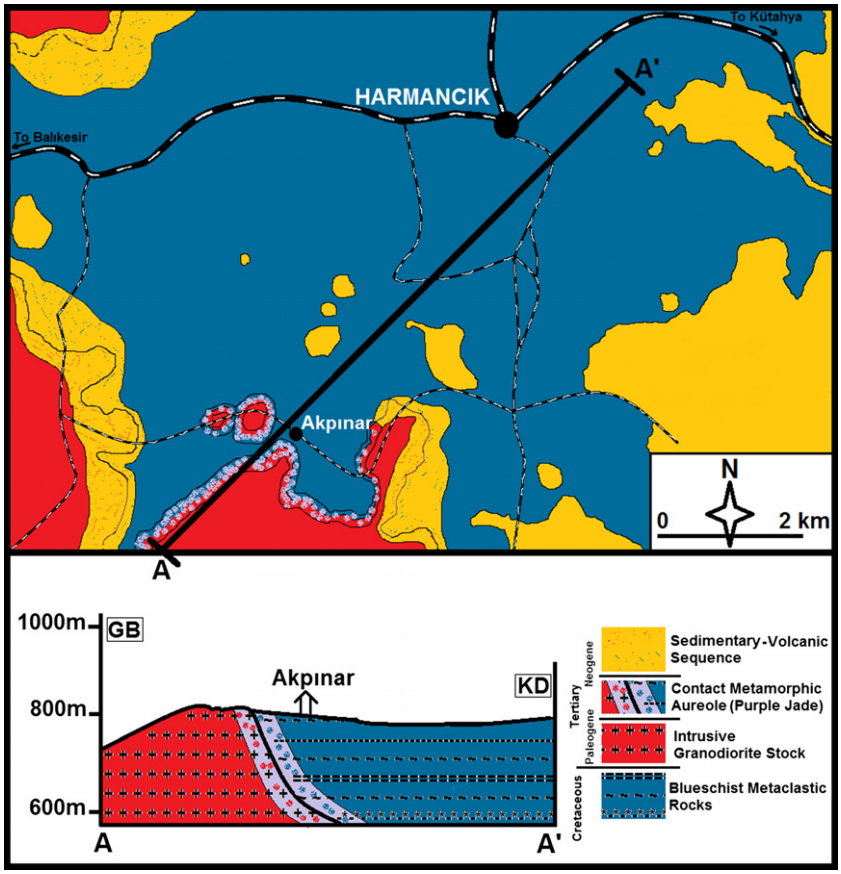

Fig. 2. Simplified geological map and its cross-section of the immediate vicinity of the village of Akpınar in the Harmancık–Bursa region (Turkey) (modified and inferred from Kaya et al. (1989) and Okay (1997, 2002)).

(2) a granodiorite, and (3) a sedimentary-volcanic sequence. The unique purple gem material occurs in an extensive contact metamorphic aureole at the border between the blueschist metaclastic rocks and the intrusive granodiorite stock (Fig. 2). Note that the first and second units have been lumped into the well-known Tavşanlı Zone by many authors (Sengör and Yilmaz, 1981; Bingöl et al., 1982; Okay, 1997, 2002; Yilmaz et al., 2010).

In previously published studies, two important geological aspects – age and depositional features – have been determined in the region (Kaya et al., 1989; Okay and Kelley, 1994). First, phengite Rb–Sr and Ar–Ar data from some rocks of the blueschist metaclastic rocks indicate that the complex has been dated as Late Cretaceous (80 ± 5 Mya) for the high pressure/high temperature (HP/LT) metamorphism (Sherlock et al., 1999). Secondly, the metamorphic complex has been separated into two main sequences, separated by a tectonic unconformity; the first sequence consists of metapelitic schists at the bottom, marbles in the middle, and a series of metabasites, metacherts, and phyllites at the top (Okay, 1980, 1984). The overlying second sequence consists of basalts, radiolarian cherts, and pelagic shales (Okay, 1997, 2002; Sherlock et al., 1999). Okay has stated that the Tavşanlı Zone constitutes one of the largest and best preserved glaucophane-lawsonite blueschist belts in the world, with regional distribution of jadeite, lawsonite and glaucophane. Specifically, the blueschist metapelites in the zone have jadeite, lawsonite, chloritoid and glaucophane; purple jades containing jadeite, K-feldspar and lawsonite (Okay, 2002).

Similar paragenesis including jadeite crystallization has been reported in the many previously published papers so far.

In the case of USA; the pyroxenes in the blueschist facies of California without jadeites (Coleman and Clark, 1968) has been reported. Moreover, Coleman has been studied jadeite deposits of the Clear Creek area, New Idria district, San Benito County, California (Coleman, 1961) and also, Coleman and his colleague have been investigated the glaucophane-bearing metamorphic rock types of the Cazedero area, California (Coleman and Lee, 1963). However, Brothers and Grapes have studied the structural and chemical variations in pyroxenes to find out which conditions caused jadeite crystallization, and reported the clastic lawsonite, glaucophane, and jadeite pyroxene in Franciscan metagraywackes from the Diablo Range, California (USA) (Brothers and Grapes, 1989). In addition, the neoblastic jadeitic pyroxene in Franciscan metagraywackes from Pacheco Pass in the central Diablo Range of California has been studied for its implications and metamorphism conditions by Ernst and Banno (1991).

In the case of Japan; Chihara has reported the jade in Japan (Chihara, 1991), jadeite in Japan (Chihara, 1999), and also mineralogical and petrographical features of jadeites from the Omni-Kotaki area, central Japan (Chihara, 1971).

In the case of Europe; jadeite-bearing metagranites in Mount Mucrone area, Sesiap Lanzo Zone, western Italian Alps has been studied in detail by Compagnoni and Maffeo (1973). In addition, D'Amico and his colleagues have stated the eclogites and jades as prehistoric implements in Europe, as a case of petrology applied to cultural heritage (D'Amico et al., 1995). Essene has been reported that relatively pure jadeite occurs in the siliceous Corsican gneiss (Essene, 1969).

This metamorphic sequence of the Tavşanlı Zone was, then, cut by two large granodioritic intrusive bodies (Bingöl et al., 1982) called the Orhaneli and the Topuk stocks (Okay, 2002) These consist of quartz, plagioclases, orthoclase, hornblendes, and biotite, and belong to the Tavşanlı Zone as well (Fig. 2). Dating based on the Ar—Ar technique of the granodiorites (Okay, 1997) has indicated that the stocks were introduced upwards into the blueschist metaclastic rocks during the Early and Middle Paleogene (Paleocene and Eocene) Period (65–37.8 Mya) of Tertiary. In addition, analysis of the hornblende mineral varieties indicates that these intrusives originated about 10 km below the current topography of the region (Bingöl et al., 1982; Okay, 1984, 2002). Since the granodiorite stocks do not show detectable deformation structures, their upward intrusion into the blueschist metaclastic rocks must have occurred after the collision of two blocks from the two sides of the Tethyan Ocean that took place in the Early Paleogene Period.

During the Late Paleogene (Oligocene) Period (37.8–23 Mya) of Tertiary, an extensive contact metamorphic aureole having a silica rich calc-alkaline chemical content (Table 2) formed at the border between the blueschist metaclastic rocks and the intruded granodiorite stock (Fig. 2). This secondary contact metamorphic aureoletic mass is the host rock for the interesting and unique gem material called "Turkish purple jade" on the worldwide gem market. This aureoletic zone has also a mineral assemblage consisting mainly of jadeite, quartz, orthoclase, epidote, chloritoid, and phlogopite according to X-ray diffraction pattern (Fig. 3) and polarized-light microscope images (Fig. 4). X-ray diffractometry (XRD) is used to identify the mineral assemble in the heterogeneous purple jade mass. Accordingly, numerical data (Table 1) obtained from XRD analysis of the representative Turkish purple jadeite sample were matched to those of the base building minerals of the metamorphic aureoletic zone using a comparative matching technique. These mineral components were labeled to aid the readers as quartz, jadeite, orthoclase, epidote, chloritoid, and phlogopite on the X-ray diffraction pattern (Fig. 3). The ideal XRD data of these minerals for comparison to the investigated samples were compiled from several crystal structure databases (AMCSD, 2011; RRUFF, 2011; WEBMINERAL, 2011). Accordingly, the three important peaks values of these components are as follows;

- 3.34(100), 4.26(22), 1.82(14) for quartz [SiO_2],
- 2.83(100), 2.42(90), 2.92(80) for jadeite [$NaAl(Si_2O_6)$] (member of the clinopyroxene group)
- 3.18(100), 4.02(90), 3.80(80) for orthoclase [$KAlSi_3O_8$] (member of the feldspar group)
- 2.91(100), 2.55(50), 3.49(44) for epidote [$CaPbSrMn^{2+}Al_2Fe^{3+}(SiO_4)(Si_2O_7)O(OH)$]
- 4.46(100), 2.46(90), 2.40(85), 2.98(80) for chloritoid [$Fe^{2+}MgMn^{2+}Al_4Si_2O_{10}(OH)_4$]
- 9.99(100), 2.61(53), 5.00(30) for phlogopite [$KMg_3AlSi_3O_{10}F(OH)$] (member of the mica group).

However, the positions of peaks with d-spacings (Å) and relative intensities [%(I/Imax)] are labeled for $\geqslant$4% of 2-theta values below 70°. The labels of overlapped peaks are in the order of relative intensities [%(I/Imax)] (Fig. 3). In this study, the petrographic observations of thin sections of the Turkish purple jade with a polarized-light microscope (Fig. 4) show that at least 40% of the gem material of the contact metamorphic aureole consists of jadeite crystallization with high relief and dark greenish-gray color. In some places jadeite comprises more than 40% of the volume. The other major mineral species present are quartz, orthoclase, epidote, chloritoid, and phlogopite, along with some opaque minerals. The analyses of chemical bulk and trace element are consistent with such a mineral paragenesis, especially higher Mn, Na, Ca, and K contents (Table 2). As a result, these purple-colored masses should not be considered pure, fine-grained purple jadeite.

Okay (1980, 1984, 1997) reported that the jadeite content in thin sections ranges from 34% to 85% and the K-feldspar content from 43% to none; in general, the higher the percentage of jadeite, the lower the percentage of K-feldspars. Similar values were also stated by Digennaro et al. (1997).

Turkish purple jade is found as massive fine-grained blocks. They have an opaque appearance and generally a pale purple color (Fig. 1C and D). In general the unique pale purple coloration of the material is a result of the mixing of the colors of these main

Table 2
Average chemical bulk and trace element analyses of the Turkish purple jade samples from the Harmancık–Bursa region (Turkey). The significant concentrations of some main building elements, such as Al, Ca, Na, K, P, Sr, and Ba can be attributed to a calc-alkaline formation environment. In addition, significant concentrations of some trace elements, such as Fe, Cr, Mn, Be, Cu, Ga, La, Nb, Ni, Pb, and Zn are characteristics of the Turkish purple jade. Some of them certainly are responsible for the production of both unique purple coloration and the characteristic Raman bands.

Oxides %	Instrument (XRF) Detection limits (%)	Sample **Turkish purple jade**	Elements	Instrument (ICP-AES) Detection limits	Sample **Turkish purple jade**
SiO_2	0.01	63.54			
Al_2O_3	0.01	20.17	Al	10 ppm	85,200
Fe_2O_3	0.01	1.78	Fe	10 ppm	11,400
CaO	0.01	2.70	Ca	10 ppm	16,800
MgO	0.01	0.35	Mg	10 ppm	1800
Na_2O	0.01	6.71	Na	10 ppm	45,500
K_2O	0.01	1.74	K	10 ppm	13,400
Cr_2O_3	0.01	<0.01	Cr	1 ppm	19
TiO_2	0.01	<0.01	Ti	0.01 ppm	<0.01
MnO	0.01	0.22	Mn	5 ppm	1540
P_2O_5	0.001	0.048	P	10 ppm	200
SrO	0.01	0.03	Sr	1 ppm	227
BaO	0.01	<0.01	Ba	10 ppm	80
LOI	0.01	2.57			
Total	0.01	**99.86**			
			Ag	0.5 ppm	<0.5
			As	5 ppm	10
			Be	0.5 ppm	4.7
			Bi	2 ppm	<2
			Cd	0.5 ppm	<0.5
			Co	1 ppm	1
			Cu	1 ppm	23
			Ga	10 ppm	40
			La	10 ppm	80
			Mo	1 ppm	<1
			Nb	1 ppm	72
			Ni	1 ppm	49
			Pb	2 ppm	15
			S	0.01 ppm	<0.01
			Sb	5 ppm	<5
			Sc	1 ppm	1
			Th	20 ppm	20
			Tl	10 ppm	<10
			U	10 ppm	20
			V	1 ppm	3
			W	10 ppm	<10
			Zn	2 ppm	95

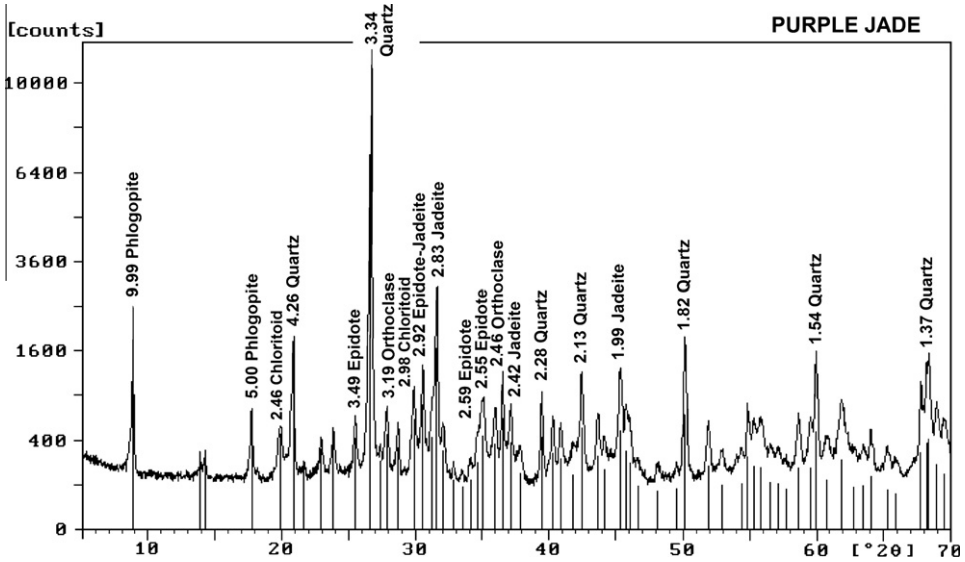

Fig. 3. The XRD pattern of a representative Turkish purple jade sample, corresponding to the numerical experimental XRD data in Table 1. The labels of the single or overlapped peaks give the basic mineral components of the purple jade-bearing contact metamorphic aureole with a mineral assemblage consisting of mainly quartz, jadeite, orthoclase, epidote, chloritoid, and phlogopite in the Harmancık–Bursa region (Turkey). The positions of peaks with d-spacings (Å) and relative intensities [%(*I*/*I*max)] are labeled for $\geqslant$4% of 2-theta values below 70°.

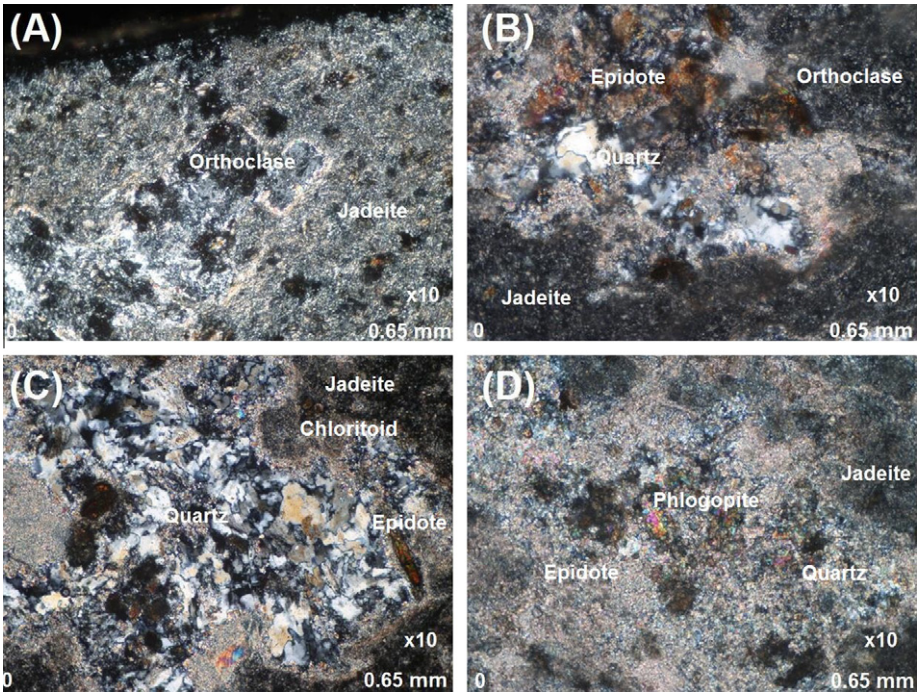

Fig. 4. Microphotographs of the representative Turkish purple jade, viewed in crossed-polarized light (magnification, 10×). The main constituents are jadeite–orthoclase (A), jadeite–quartz–epidote–orthoclase (B), jadeite–quartz–epidote–chloritoid (C), and jadeite–quartz–epidote–phlogopite (D). It is seen that at least 40% of the volume of the extensive contact metamorphic aureole consists of observable jadeite crystallization with high relief and dark greenish-gray color; the volume of jadeite is over 60% in some places, In addition, there exist less important opaque minerals in the thin-sections. The width of the images is 0.65 mm. (For interpretation of the references to color in this figure legend, the reader is referred to the web version of this article.)

component minerals. However, some parts of the samples display whitish (quartz-rich portions and veins) and/or yellowish (quartz and orthoclase-rich portions and veins) colorations. Therefore, it can be assumed that in these parts of the samples, the abundance of jadeite is relatively lower.

Finally, a sedimentary and volcanic sequence with many fragments of the debris flows is unconformably settled down at the top of the region (Fig. 2). The sequence has been dated as Neogene Period (23–3.5 Mya) in many previously published papers (Sherlock et al., 1999; Okay, 2002; Yilmaz et al., 2010).

3.2. Specific gravity measurements

The hydrostatic balance (HB) method was used to analyse the Turkish purple jade samples with three different colorations. The values based on the formula ($SG = W_{air}/W_{air} - W_{water}$), were measured to be 3.05 in the intensely purple colored part, 3.02 in the pale purple and whitish mixed colored part, and 2.69 in the whitish and yellowish colored part (Fig. 5). These results support the conclusions above since jadeite is the heaviest of the three major mineral components (SG = 3.24–3.42) quartz is lighter (SG = 2.65) and orthoclase lighter still (SG = 2.53–2.56).

However, since the minor whitish and yellowish parts of the material are not used for gemstones, the average specific gravity value of the Turkish purple jade is 3.04.

In fact, this specific gravity value is unusual for jades composed of jadeite worldwide. Rather, the value is very similar to those of the jades composed of nephrite. In the literature, it has been proposed that the specific gravity range of the nephrite jades is 2.90–3.02. By contrast, well-known jadeite jades have a specific gravity range of 3.3–3.5 (Htein and Naing, 1994). The typical specific gravity of Turkish purple jade is thus distinctive—a bit too high for nephrite and much too low for jadeite. Therefore the hydrostatic balance method is a powerful tool to distinguish the Turkish purple jades from the other natural and synthetic jades.

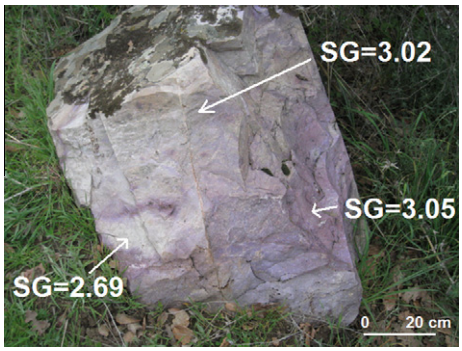

Fig. 5. Specific gravity (SG) values of the Turkish purple jade material with three different colorations—this is a large block of the extensive contact metamorphic aureole. The values, based on the formula ($SG = W_{air}/W_{air} - W_{water}$), were measured to be 3.05 in the intensely purple colored part, 3.02 in the pale purple and whitish mixed colored part, and 2.69 in the whitish and yellowish colored part. (For interpretation of the references to color in this figure legend, the reader is referred to the web version of this article.)

3.3. Chemical constituents and confocal micro-Raman vibrational bands

Chemical analyses of the representative intensely purple colored Turkish jade samples were carried out using both X-ray fluorescence (XRF) for major oxides and inductively coupled plasma-atomic emission microscopy (ICP-AES) for trace elements, and their chemical constituents are given in order in Table 2.

Some rock building elements, such as Al, Ca, Na, K, P, Sr, and B of which characterize an acidic rock formation, and trace elements, such as Fe, Cr, Mn, Be, Cu, Ga, La, Ni, Pb, and Zn are remarkable high ratios. Hence, chemical impurities in the Turkish purple jade are present at significant concentrations for Fe (1.14%), Mn (1540 ppm), Be (4.7 ppm), Zn (95 ppm), Ni (49 ppm), Cu (23 ppm),

Cr (19 ppm), and Pb (15 ppm) as transition metal elements, and for La (80 ppm) as a rare earth element, and Ga (40 ppm) as a metalloid element (Table 2). Accordingly, we can interpreted that pale purple coloration of this jade is owing to rich Mn^{3+} ions replacing a large number of Al^{3+} ions in the mass during the blueschist metamorphic facies formation in the region.

In addition, the result of the chemical bulk analysis indicates that the Turkish purple jade has significant concentrations of some main elements, such as Al, Ca, Na, and K as well as P, Sr, and Ba. In fact, these relatively higher ratios are important indicators for igneous rock formations of acidic character. On the other hand, these relatively higher ratios mean that this unique material cannot be represented by a chemical formula like the ideally-known clinopyroxene composition [$Na(Al,Fe)Si_2O_6$], where chemical substitutions of Na (in the M2, Al (in the M1 site), or Si (in the tetrahedral site) are possible (Prewitt and Burnham, 1966; Htein and Naing, 1994; Zhao et al., 1994; Nestola et al., 2007).

The dispersive confocal micro-Raman spectra of the Turkish purple jade including vibration bands between 1600 and 50 cm^{-1} are given as the single spectrum including the bands characterized as mainly jadeite (Fig. 6), as the mapped multi-spectra and related microscope images of them (Fig. 7), and as the compared and contrasted combined spectra of them (Fig. 8).

It is important that the micro-Raman vibrational bands of the Turkish purple jade have not been reported previously in the references related to jadeite-jade or nephrite-jade. Therefore, a total of 20 Raman bands characteristic of the Turkish purple jade were established even though some of them are close together values and their causes were inferred (Table 3). These spectra have more peak numbers than those of other colored kinds of the jadeite-jades which have been reported by Zhao et al. (1994), Gendron et al. (2002), Nestola et al. (2007), Bersani and Lottici (2010), and Fan et al. (2009), even though many of the peaks match exactly those of the Turkish purple jade.

As a result, the dispersive confocal micro-Raman bands centered at 1444, 1300, 1038, 984, 876, 776, 697, 571, 521, 464, 430, 372, 326, 307, 264, 218, 201, 143, 126, and 101 cm^{-1} are characteristic of the Turkish purple jade (Table 3). Moreover, the underlined ones are very strong bands.

Interpretation of the whole micro-Raman analysis for Turkish purple jade must take into account that at least 40% of the fine-grained material is jadeite (Fig. 2), but significant amounts of quartz, orthoclase, chloritoid, phlogopite, epidote, and opaque minerals are also present (Figs. 3 and 4).

Smith has been interpreted that the Si—O—Si symmetric stretching vibration of jadeite is affected by the nature of the M2 cation and, to a lesser extent, by the M1 cation: the wave number of the corresponding spectral band (in the 650–750-cm^{-1} range) may give indirect "chemical" information on the actual composition, after suitable calibration (Smith, 2005). As a result, the jadeite or nephrite nature of jade Chinese artifacts from the Trésor of the Muséum National d'Histoire Naturelle in Paris was determined by means of Raman spectroscopy: distinguishing features are the Si—O—Si stretching vibration at 675 cm^{-1} (nephrite) and above 695 cm^{-1} (jadeite), and the presence of OH stretching vibrations for nephrite (Smith, 2005; Bersani and Lottici, 2010).

A normal coordinate of the form $Q = Q_0\cos(2\pi\nu n_{vib}t)$, which is actually a linear combination of bond lengths and bond angles, is associated with each normal mode. Depending on the dominant term in the normal coordinate, these modes can be classified as either stretching (n), bending (d), torsional (t), librational (R0/T0 pseudorotations/translations) or lattice modes (the latter include the relative displacement of the unit cells) (Gouadec and Colomban, 2007; Colomban and Prinsloo, 2009; Slodczyk and Colomban, 2010; Vandenabeele, 2010).

These experimental data (Table 3) (Figs. 6–8) of the Turkish purple jade indicate that the formation of distinctive vibrational bands is definitely related to lattice defects which can be attributed to some chemical impurities (external defects) and structural imperfections (internal defects) according to the symmetry and main activity of SiO_4 tetrahedron with Td symmetry and with C_{2v} symmetry in a D_{6h} structure (Colomban and Prinsloo, 2009).

The first most intensive and widest Raman band peaked at 697 cm^{-1} and can be interpreted as being ν_2 doubly symmetric bending mode of (SiO_4/M) centers. The "M" includes the some cationic substitutions of Si by Fe, Cr, Mn, Be, Cu, Ni, Pb, and Zn, and also K and Na. The second most intensive and widest Raman band peaked at 372 cm^{-1} can be interpreted as being ν_2 single symmet-

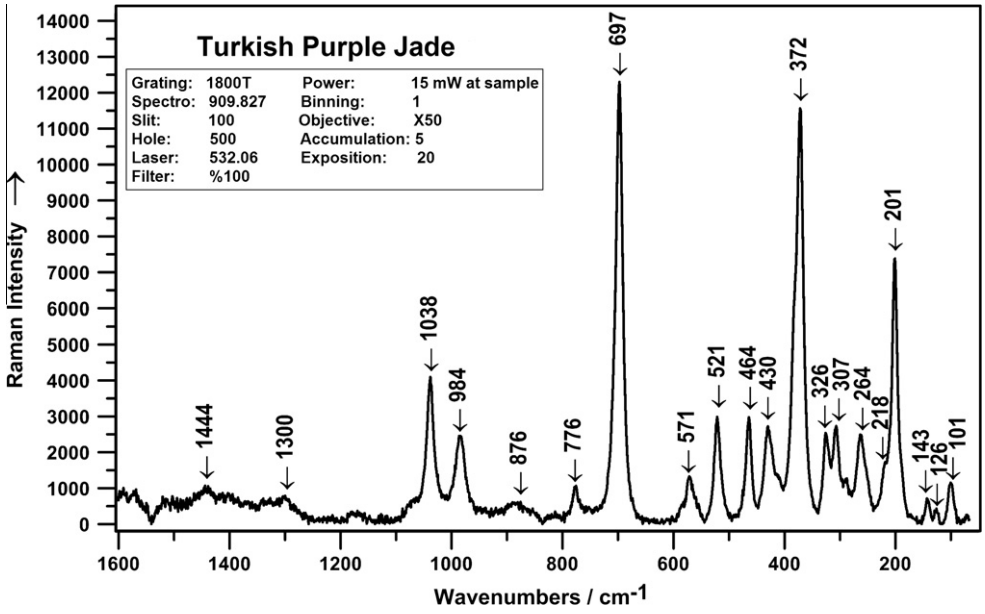

Fig. 6. Micro-Raman vibrational bands of the Turkish purple jade that constitutes a large portion of an extensive contact metamorphic aureole. The bands peaking at 1038, 697, 372, and 201 cm^{-1} represent the mineral jadeite (clinopyroxene subgroup) and are distinctive. The spectrum shows stretching and bending modes equivalent to those of polyhedral (mostly tetrahedral or octahedral) isolated molecules. The difference becomes clear by the cations generating T (translational) and R (rotational) libration modes.

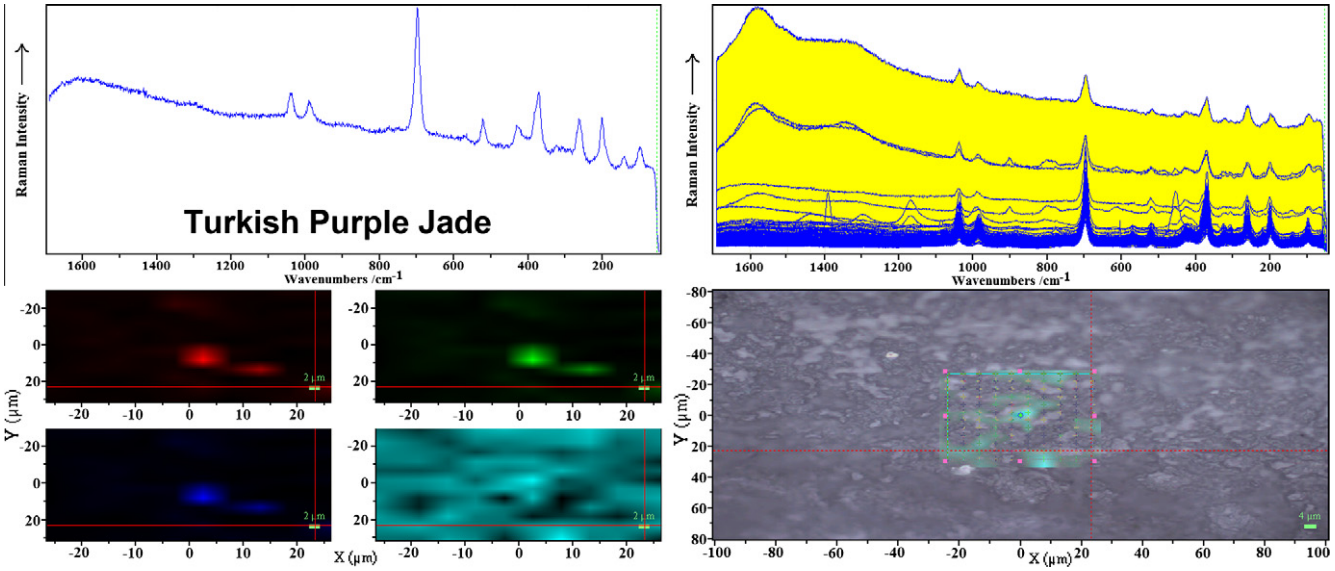

Fig. 7. The mapped multi-spectra and related microscope image of Fig. 6. They show the variation of any fitted parameter (i.e. intensity, width or position of one band) as a function of the point of analysis. If the mapping is regular and sufficiently tight, one gets a "smart map" of the parameter (color or contrast scaling) superimposed with the optical image of the probed area. (For interpretation of the references to color in this figure legend, the reader is referred to the web version of this article.)

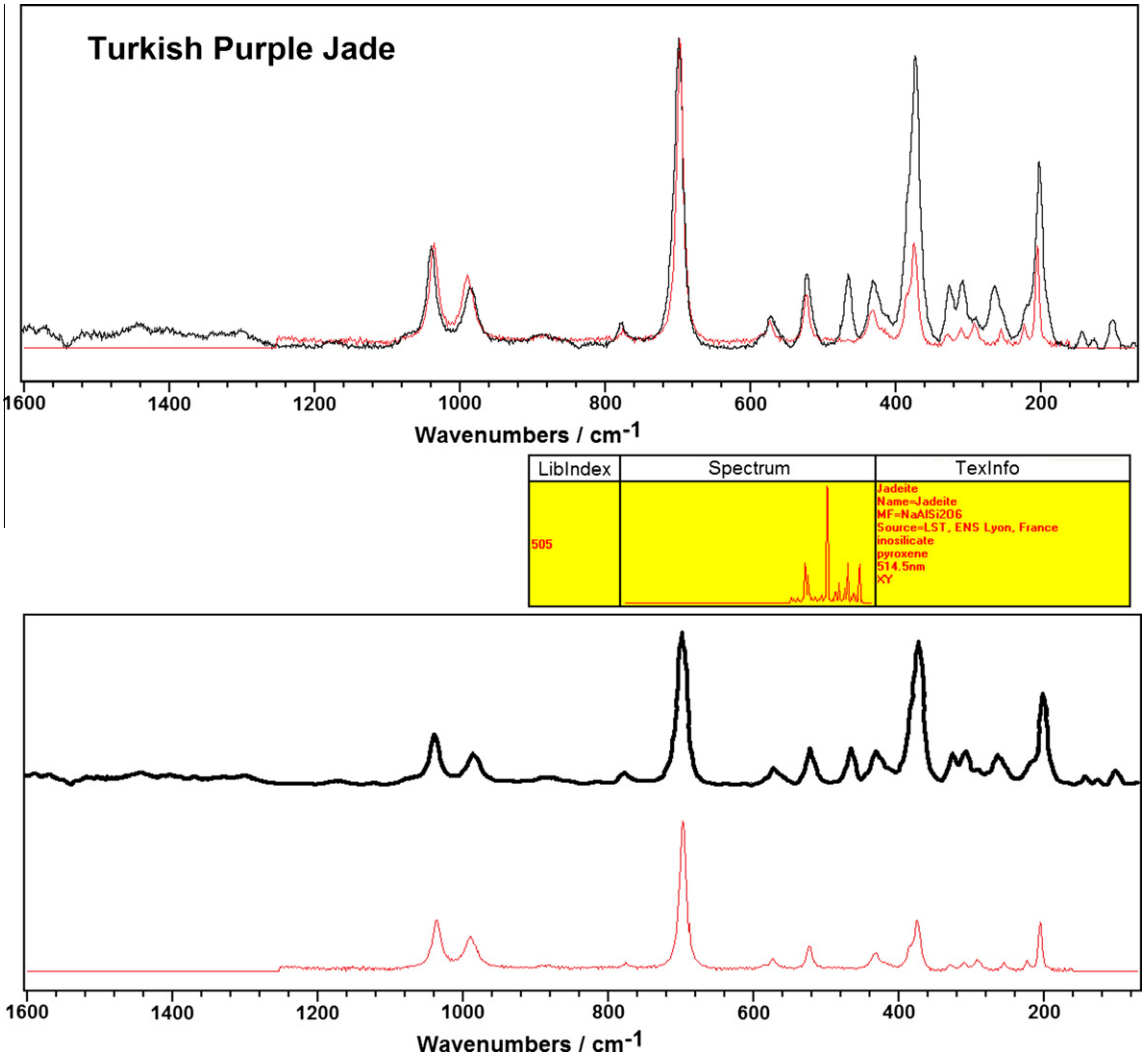

Fig. 8. Comparison of the spectrum of the micro-Raman bands in Fig. 6 for Turkish purple jade (black traces) with those of pure jadeite from anywhere (red traces). (For interpretation of the references to color in this figure legend, the reader is referred to the web version of this article.)

Table 3
Confocal micro-Raman vibrational bands of the unoriented sample of the representative Turkish purple jade from the Harmancık–Bursa region (Turkey), and their inferred causes according to symmetry and main activity of SiO_4 tetrahedron.

Peak number	Micro-Raman bands wavenumbers/cm^{-1}	Inferred causes
1	1444	Non-bridging oxygen hole centers with several precursors (i.e. peroxy linkage) and oxygen vacancy
2	1300	Non-bridging oxygen hole centers with several precursors (i.e. peroxy linkage) and oxygen vacancy
3	1038	v_1 doubly symmetric stretching modes of (SiO_4/M) centers
4	984	
5	876	v_1 doubly symmetric stretching modes of degeneracy of (SiO_4/M) centers
6	776	
7	697	v_2 doubly symmetric bending mode of (SiO_4/M) centers The "M" includes the some cationic substitutions of Si by Fe, Cr, Mn, Be, Cu, Ni, Pb, and Zn, and also K and Na
8	571	v_2 fourthly symmetric bending modes of degeneracy of (SiO_4/M) centers
9	521	
10	464	
11	430	
12	372	v_2 single symmetric bending mode of (SiO_4/M) centers
13	326	Rotational libration mode
14	307	Rotational libration mode
15	264	Rotational libration mode
16	218	Rotational libration mode
17	201	Translational libration
18	143	Translational libration mode
19	126	Translational libration mode
20	101	Translational libration mode

ric bending mode of (SiO_4/M) centers. The third most intensive and widest Raman band peaked at 201 cm^{-1} can be interpreted as translational libration. Finally, the fourth distinctive Raman band peaked at 1038 and 984 cm^{-1} can be interpreted as being ν_1 doubly symmetric stretching modes of (SiO_4/M) centers.

Fig. 6 shows that both sides of these bands were barricaded with some crystalline defect structures (imperfections) (Table 3).

According to dispersive confocal micro-Raman spectroscopy (DCμRS) in combination with quantitative analysis performed by ICP-AES, Their productions are mainly ascribed to the presence of relatively higher concentrations of some transition metal elements, such as Fe, Cr, Mn, Be, Cu, Ni, Pb, and Zn in (SiO_4/M) centers, which can be attributed to extrinsic defects (chemical impurities) derived from the intrusive granodiorite that gave rise to the contact metamorphic aureole in the region. Since, it is well-known that elements with high atomic numbers that are situated on the right side of the periodic table (covalent materials in general) are good Raman scatters whereas ionic structures are difficult to analyse with Raman spectroscopy. Some transition metal ions from the 3*d* (chromium) or 4*f* (lanthanides) groups produce strong fluorescence signals which often mask the Raman spectra but can be used for short range structure and/or residual stress assessment (Gouadec and Colomban, 2007; Colomban and Prinsloo, 2009; Vandenabeele, 2010).

Meanwhile, they are caused by the presence of relatively higher concentrations of some main building elements, such as Na and K in (AlO_4/M^+) and (SiO_4/M^+) centers, which can be attributed to extrinsic defects (chemical impurities), and additionally, to intrinsic defects (the nonbridging oxygen deficient centers with several precursors, self-trapped exciton, and dislocations) resulting from the long and strong metamorphism conditions during the Tertiary.

Some main building elements of the Turkish purple jade indicate that the bands in the spectra can be mainly attributed to extrinsic defects (chemical impurities) which are due to increasing amounts of tetrahedral character with increasing electron density caused by the presence of trace elements, taking into consideration the increased ionic character of the Si—O bonds in the alkali silicate, and can be partially attributed to intrinsic defects (the nonbridging oxygen deficient centers with several precursors and self-trapped exciton). Nutall and Weil (1980) reported a hydrogenic trapped hole-center with four hydrogen atoms in a regular silicon lattice position. Since, in the case of some elements, compensation of the electric charge is necessary, additional cations such as H, Li, Na, K, and Ag can be incorporated in inter-lattice positions in conjunction with structural channels. However, the contribution of ionic bonds like Al—O is null according to that of covalent Si—O bonds (Colomban and Prinsloo, 2009). So, the considerable strength of the Si—O bond results in a high melting temperature (Colomban and Prinsloo, 2009). The basic unit of a silicate, the SiO_4 tetrahedron, is a strong chemical entity and the possibility to share oxygen atoms between two tetrahedra with variable Si—O—Si angles or to have non-bridging oxygen atoms gives a polymeric character to silicates (Colomban and Prinsloo, 2009). The (SiO_4) Center is caused by substitution for Si^{4+} with an electron hole at one of the four nearest O^{2-} ions, forming O^-. The non-bridging oxygen hole center (≡Si—O) is described as a hole trapped in a single oxygen atom bound to a single silicon on three oxygen atoms in the SiO_2 structure (Weil, 1984). Oxygen excess centers include the peroxy radical (≡Si—O—O), an oxygen associated hole centers consisting of an O^{2-} ion bonded to single silicon on three oxygen atoms, and the peroxy linkage (≡Si—O—O≡). Because of the negative net charge, additional trivalent substitutes of the Si^{4+} positions occur as charge compensation (i.e. Al^{3+}) in such a way that an additional proton is bound on the Al^{3+} (Colomban and Prinsloo, 2009; Vandenabeele, 2010).

Slodczyk and Colomban have stated that many electrical/electrochemical/magnetic properties result from a competition between different potentials of the chemical bonding and structure. In generals, some atoms (alkali and earth alkali cations) have a strong ionic character. Some other atoms develop covalent bonding (i.e. transition metals) and form strong "molecular" bricks. Metallic bonds can also be formed between atoms such as Ag, Cu, Tl, and ionized clusters intermediately between ions and complex nanoclusters may be observed (Slodczyk and Colomban, 2010).

In granitic rocks, green- and white-colored jadeite-jade occurrences are rare (Bersani and Lottici, 2010); however, purple colored jade occurrence is the rarest. Hence, granites and similar host rocks have been intensely reworked by post-magmatic and host-rock fluids, resulting in intense re-crystallization, enrichment in Na, Al, Fe and rare elements, and replacement of primary muscovite and sodic–calcic clinopyroxenes (i.e. diopside) in order to produce typical single-jadeite crystallization [$Na(Al,Fe)Si_2O_6$] (Rossi et al., 1983; Brizi and Mellini, 1992; Nestola et al., 2007).

In addition, micro-Raman spectroscopy has been used to investigate bleached and filled jadeite jade: bleaching with strong acid

Table 4
A simple comparison of the purple and lavender jadeite in terms of color appearance, cause of color, and basic gemmological properties.

Properties	Purple jadeite	Lavender jadeite
Color appearance	Pale purple	Vivid lavender
Possible cause of color	Fe Zn Ni Mn	Mn (mainly)
Specific gravity	3.04	3.32
Luminescence	Inert	Weak greenish
Characteristics	• Under the yellow light, purple jadeite may look same color • Purple jade is always opaque	• Under the yellow light, lavender jadeite may look slightly darker than it is • It is difficult to find dark lavender jadeite with good transparency and fine texture • Normally lavender jadeite is classified into three types, namely pinkish lavender, bluish lavender and eggplant lavender

produces micro-cracks, which are filled with epoxy resin, evidenced by the Raman shifts close to 777, 1123, 1611, 2930, and 3065 cm^{-1}. Moreover, it is possible to identify bleached jade by distinguishing resin from paraffin (Fan et al., 2007, 2009; Bersani and Lottici, 2010). In particular, Fan and his colleagues have been stated a research conducted using a NIR Raman spectrometer for a large number of jadeite samples, and they have reported that NIR (785 nm) Raman spectrometer exhibits advantage of non-destruction, quickness, accurateness, and weak fluorescence interferences (Fan et al., 2007, 2009).

On the other hand, the results of the chemical trace element analysis, which show some transition metal elements such as Fe, Cr, Mn, Be, Cu, Nb, Ni, Pb, and Zn, metalloid element such as Ga, and rare-earth element such as La, indicate that higher presence of constitutive trace elements is one of the most important characteristics of the Turkish purple jade. Some of them are certainly responsible, as external lattice defects, for producing the unique purple color. The colors of all kinds of jadeite-jades are due to the presence of impurity elements, as reported in previous papers (Harder, 1995). For example, the presence of iron and/or chromium imparts a green color to the mineral (Rossman, 1974). Manganese provides a lavender color (Nassau and Shigley, 1987; Fan et al., 2007, 2009). However, the unique purple coloration of the Turkish jade is due to a more complex mechanism, since many transition metal coloration agents are present in it. In order to clarify the purple color formation, further investigation will be necessary.

However, while Turkish "purple" jadeite jade appears unique, it is well-known that 'lavender' jadeite jade is found in several localities, including Myanmar, Japan, New Zealand, and some South American's countries. Therefore, it is quite valuable. A simple comparison table of both purple and lavender jadeite in terms of color appearance, cause of color, and basic gemmological properties is given in Table 4.

4. Conclusions

From the region comprising the Harmancık–Bursa region in Turkey, some tons of the purple-colored jade material that occur a metamorphic zone at the border between a coherent blueschist metamorphic sequence and an intrusive granodiorite have been commercially exploited, and exported as specifically named "Turkish (and/or Turkish purple jade" since the 1980s.

However, the purple jade deposit is not currently being mined officially at this one locality in Turkey (Harmancık–Bursa region) because of some economical reasons. However, the material has been extracted and exported illegally for a long time. This acquirement is estimated as an amount of 10 tons per year. On the other hand, according to field studies on the deposit, the potential reserve of purple jade mass is about 5,000,000,000 tons for one meter dept, about 2.5 km length and about 2 km width. As a result, we can propose that purple jade occur in sufficient quantity to support a jewellery market.

Dispersive (visible) confocal micro-Raman spectroscopy (DCμRS) was used to characterize unique gem rough from an extensive metamorphic aureole in Turkey. A confocal micro-Raman spectrometer and a hydrostatic balance are the most accurate non-destructive and non-invasive tools to distinguish natural Turkish purple jades from other colored natural and synthetic jades and to identify their provenance regarding geographic region. Thus, it is proposed that confocal micro-Raman spectroscopy could play a much more important role in the gemmology field.

Turkish purple jade samples are found as large, fine-grained masses. They have an opaque appearance and generally a pale purple color. With the dual correlated use of destructive conventional petrographic analysis with a polarized-light microscope and non-destructive confocal micro-Raman spectroscopy, this study established the detailed accuracy of confocal micro-Raman spectroscopy in analyzing both rough and polished Turkish purple jade. The resulting characterization appears to be unique to material from the Turkish occurrence, which is the only known source of purple jade comprised largely of jadeite instead of nephrite. The dispersive confocal micro-Raman spectroscopy (DCμRS) was performed on the Turkish purple jade, and possible causes of the vibrational bands were attributed to some crystalline defects (impurities and imperfections) with reference to the ICP-AES analysis. These vibration bands can be mainly attributed to extrinsic defects (chemical impurities) due to increasing amounts of tetrahedral character with rising electron density caused by the presence of trace elements, taking into consideration the increased ionic character of the Si—O bonds in the alkali silicate, and can be partially attributed to intrinsic defects (the non-bridging oxygen-deficient centers with several precursors and self-trapped exciton). They are mainly ascribed to the presence of relatively higher concentrations of some transition metal elements, such as Fe, Cr, Mn, Be, Cu, Nb, Ni, Pb, and Zn in (SiO_4/M) centers which can be attributed to extrinsic defects (chemical impurities) derived from the contact metamorphic aureole stock in the region. At the same time, we can interpret that pale purple coloration of this jade is due to rich Mn^{3+} ions replacing a large number of Al^{3+} ions in the mass during the blueschist metamorphic facies formation in the region.

The rapid mapping capabilities allow for large scale survey maps to be collected with smaller higher spatial resolution maps obtained once a region(s) of interest has been located. This technology has been used to investigate the Turkish purple jade.

Acknowledgements

This study is a part of the thesis prepared for the B.Sc., of the second author. The confocal micro-Raman spectrometer device

was purchased with the grant of the BAP project, numbered BAP-2009.KB.FEN.051, of Dokuz Eylül University. In addition, the authors wish to give great thanks to Prof. Dr. R. Sami AKSOY, Prof. Dr. I. Hakkı BAHAR, Cengiz HEPİYİLER, and Prof. Dr. Necdet TÜRK for their help and support procuring the spectrometer device. Ultimately, thank you to referees' for constructive review, recommendations, and patience.

References

Adamo, I., Pavese, A., Prosperi, L., Diella, V., Ajò, D., Dapiaggi, M., Mora, C., Manavella, F., Salusso, F., Giuliano, V., 2006. Characterization of omphacite jade from the Po Valley, Piedmont, Italy. Journal of Gemmology 30, 215–226.

AMCSD, 2011. American Mineralogist crystal structure database by Downs et al. (1993) via http://www.minsocam.org/MSA/Crystal_Database.html, and http://rruff.geo.arizona.edu/AMS/amcsd.php.

Andrews, E.W.V., 1986. Olmec jades from Chacsinkin, Yucatan, and Maya ceramics from La Venta, Tabasco. In: Wyllys Andrews, E., V (Ed.), Research and Reflections in Archaeology and History: Essays in Honor of Doris Stone. Tulane University, Middle American Research Institute, New Orleans, LA.

Bersani, D., Lottici, P.P., 2010. Application of Raman spectroscopy to gemology. Analytical and Bioanalytical Chemistry 397, 2631–2646.

Biino, G.G., Compagnoni, R., 1992. Very-high pressure metamorphism of the Brossasco coronite metagranite, southern Dora Maira Massif, Western Alps. Schweiz Mineral. Petrogr. Mitt. 72, 347–363.

Bingöl, E., Delaloye, M., Ataman, G., 1982. Granitic intrusions in western Anatolia: a contribution to the geodynamic study of this area. Eclogae Geologica Helvatica 75, 437–446.

Bishop, C., Woolley, A., Kinnes, I., Harrison, R., 1977. Jadeite axes in Europe and the British Isles: an interim study. Archaelogica Atlantica 2, 1–8.

Brizi, E., Mellini, M., 1992. Kinetical modelling of exsolution textures in igneous pyroxenes: Acta Vulcanologica 2, 87–93.

Brothers, R.N., Grapes, R.H., 1989. Clastic lawsonite, glaucophane, and jadeite pyroxene in Franciscan metagraywackes from the Diablo Range, California. Geological Society of America Bulletin 101, 14–26.

Cameron, M., Papike, J.J., 1981. Structural and chemical variations in pyroxenes. American Mineralogist 66, 1–50.

Chihara, K., 1971. Mineralogy and paragenesis of jadeites from the Omi-Kotaki area, central Japan. Mineralogical Society of Japan Special Paper 1, 147–156.

Chihara, K., 1991. Jade in Japan. In: Keverne, R. (Ed.), Jade. Van Nostrand Reinhold, New York, pp. 216–217.

Chihara, K., 1999. Jadeite in Japan. Journal of the Gemmological Society of Japan. 20, 5–21.

Coleman, R.G., 1961. Jadeite deposits of the Clear Creek area, New Idria district, San Benito County, California. Journal of Petrology 2, 209–247.

Coleman, R.G., Clark, J.R., 1968. Pyroxenes in the blueschist facies of California. American Journal of Science 266, 43–59.

Coleman, R.G., Lee, D.E., 1963. Glaucophane-bearing metamorphic rock types of the Cazadero area, California. Journal of Petrology 4, 260–301.

Colomban, P., Prinsloo, L., 2009. Optical spectroscopy of silicates and glasses. In: Yatwood, J., Douthwaite, R., Duckett, S. (Eds.), Spectroscopic Properties of Inorganic and Organometallic Chemistry, vol. 40. RSC Publishing, pp. 128–149.

Compagnoni, R., Maffeo, B., 1973. Jadeite-bearing metagranite and related rocks in Mount Mucrone area (Sesiap Lanzo Zone, Western Italian Alps). Schweiz. Min. Petr. Mitt. 53, 355–378.

Crowhurst, D., 2001. Jade is jade. Colored Stone 14, 112–113.

D'Amico, C., Campana, R., Felice, G., Ghedini, M., 1995. Eclogites and jades as prehistoric implements in Europe: a case of petrology applied to cultural heritage. European Journal of Mineralogy 7, 29–41.

Delé-Dubois, M.L., Dhamelincourt, P., Poirot, J.P., Schubnel, H.J., 1986. Differentiation between gems and synthetic minerals by laser Raman microspectroscopy. Journal of Molecular Structure 143, 135–138.

Digennaro, M.A., Trossarelli, C., Rinaudo, C., 1997. Characterization of violet jade from Turkey. Zeitschrift der Deutschen Gemmologischen Gesellschaft 46 (3), 169–174.

Easby, E.K., 1991. Jade in South America and the Caribbean. In: Keverne, R. (Ed.), Jade. Van Nostrand Reinhold, New York, pp. 338–341.

Ernst, W.G., Banno, S., 1991. Neoblastic jadeitic pyroxene in Franciscan metagraywackes from Pacheco Pass, central Diablo Range, California, and implications for the inferred metamorphic *P-T* history. New Zealand Journal of Geology and Geophysics 34, 285–292.

Essene, E., 1969. Relatively pure jadeite from a siliceous Corsican gneiss. Earth and Planetary Science Letters 5, 270–272.

Fan, J.L., Guo, S.G., Liu, X.L., 2007. Application of Raman spectrometer (785 nm) to jadeite test (in Chine with English abstract), via <http://www.ncbi.nlm.nih.gov/pubmed/18306795>.

Fan, J.L., Guo, S.G., Liu, X.L., 2009. The Application of confocal micro-Raman spectrometer to nondestructive identification of filled gemstones. Spectroscopy Letters 42, 129–135.

Gendron, G., Smith, D.C., Gendron-Bdou, A., 2002. Discovery of Jadeite-Jade in Guatemala confirmed by non-destructive Raman microscopy. Journal of Archaeological Science 29, 837–851.

Gouadec, G., Colomban, P., 2007. Raman Spectroscopy of nanomaterials: how spectra relate to disorder, particle size and mechanical properties. Progress in Crystal Growth and Characterization of Materials 53, 1–56.

Hanni, H., Kiefert, L., Chalain, J.P., 1997. Raman spectroscopic applications to gemmology. Journal of Gemmology 25, 394–407.

Harder, H., 1995. Trace elements as colouring agents in jadeites. The Journal of Gemmology 24, 508–511.

Harlow, G.E., Sorensen, S.S., 2005. Jade (nephrite and jadeitite) and serpentinite: metasomatic connections. International Geological Review 47, 113–146.

Harlow, G.E., Sorensen, S.S., Sisson, V.B., 2007. Jade. In: Groat, Lee A. (Ed.), The Geology of Gem Deposits, Short Course Handbook Series, vol. 37. Mineralogical Association of Canada, Quebec, pp. 207–254.

Hatipoğlu, M., 2010. Response to jadeite from Turkey. Rocks & Minerals 85, 301.

Htein, W., Naing, A.M., 1994. Mineral and chemical compositions of jadeite jade of Myanmar. Journal of Gemmology 24, 269–276.

Kaya, O., Özkoçak, O., Lisenbee, A., 1989. Jura öncesi bloklu tortul kayaların stratigrafisi, Bursa güneyi). Bulletin of MTA (Turkey) 109, 22–32.

Lewis, I.R., Edwards, H.G.M., 2001. Handbook of Raman Spectroscopy, From the Research Laboratory to the Process Line, Practical Spectroscopy Series. Marcel Dekker Inc., New York.

Middleton, A., Freestone, I., 1995. In: Rawson, J. (Ed.), Chinese Jade. British Museum Press, London, p. 413.

Morimoto, N., 1988. Nomenclature of pyroxenes. American Mineralogist 73, 1123–1133.

Morimoto, N., 1989. Nomenclature of pyroxenes. The Canadian Mineralogist 27, 143–156.

Nassau, K., Shigley, J.E., 1987. A study of the general electric synthetic jadeite. Gems & Gemology 23, 27–35.

Nestola, F., Tribaudino, M., Ballaran, T.B., Liebske, C., Bruno, M., 2007. The crystal structures of pyroxenes along the jadeite-hedenbergite and jadeite-aegirine joins. American Mineralogist 92, 1492–1501.

Nutall, R.H.D., Weil, J.A., 1980. Two hydrogenic trapped-hole species in quartz. Solid State Communications 33, 99–102.

Okay, A.I., 1980. Mineralogy, petrology and phase relations of glaucophane-lawsonite zone blueschists from the Tavşanlı region, northwest Turkey. Contribution to Mineralogy and Petrology 72, 243–255.

Okay, A.I., 1984. Distribution and characteristics of the northwest Turkish blueschists. In: Robertson, A.H.F., Dixon, J.E. (Eds.), The Geological Evolution of the Eastern Mediterranean, vol. 17. Geological Society of London, pp. 455–466 (Special Publication).

Okay, A.I., 1997. Jadeite-K-feldspar rocks and jadeitites from northwest Turkey. Mineralogical Magazine 61, 835–843.

Okay, A.I., 2002. Jadeite–chloritoid–glaucophane–lawsonite blueschists in northwest Turkey: unusually high P/T ratios in continental crust. Journal of Metamorphic Geology 20, 757–768.

Okay, A., Kelley, S.P., 1994. Tectonic setting, petrology and geochronology of jadeite + glaucophane and chloritoid + glaucophane schists from northwest Turkey. Journal of Metamorphic Geology 12, 455–466.

Okay, A.I., Harris, N.B.W., Kelley, S., 1998. Blueschist exhumation along a Tethyan suture in northwest Turkey. Tectonophysics 285, 275–299.

Prewitt, C.T., Burnham, C.W., 1966. The crystal structure of jadeite, $NaAlSi_2O_6$. American Mineralogist 51, 956–975.

Raman, C.V., Krishnan, K.S., 1928. A new type of secondary radiation. Nature 121, 501.

Rossi, G., Smith, D.C., Ungaretti, L., Domeneghetti, M.C., 1983. Crystal-chemistry and cation ordering in the system diopside-jadeite: a detailed study by crystal structure refinement. Contributions to Mineralogy and Petrology 83, 247–258.

Rossman, G.R., 1974. Lavender jade: the optical spectrum of $Fe3^+$ and Fe^{2+}–Fe^{3+} inter-valence charge transfer in jadeite from Burma. American Mineralogist 59, 868–870.

RRUFF, 2011. Database of Raman spectroscopy, X-ray diffraction and chemistry of minerals via <http://www.rruff.info/>.

Şengör, A.M.C., Yılmaz, Y., 1981. Tethyan evolution of Turkey: a plate tectonic approach. Techtonophsics 75, 181–241.

Sherlock, S., Kelley, S.P., Inger, S., Harris, N., Okay, A.I., 1999. $^{40}Ar—^{39}Ar$ and Rb—Sr geochronology of high-pressure metamorphism and exhumation history of the Tavşanlı Zone, NW Turkey. Contributions to Mineralogy and Petrology 137, 46–58.

Slodczyk, A., Colomban, P., 2010. Probing the nanodomain origin and phase transition mechanisms in (un) poled PMN-PT single crystals and textured ceramics. Material 3, 5007–5029.

Smith, D.C., 2005. In: Edwards, H.G.M., Chalmers, J.M. (Eds.), Raman spectroscopy in archaeology and art history. RSC analytical spectroscopy monographs. Royal Society of Chemistry, Cambridge, pp. 335–378.

Smith, D.C., Gendron, F., 1997. Archaeometric application of the Raman microscope to the non-destructive identification of two Pre-Columbian ceremonial polished "greenstone" axe heads from Mesoamerica. Journal of Raman Spectroscopy 28, 731–738.

Teixeira, M.I., Melo, A.P., Ferraz, G.M., Caldas, L.V.E., 2010. Application of jade samples for high-dose dosimetry using the EPR technique. Applied Radiation and Isotopes 68, 582–585.

Tuncer-Arslanlar, Y., Garcia-Guinea, J., Kibar, R., Çetin, A., Ayvacıklı, M., Can, N., 2011. Luminescence behaviour and Raman characterization of jade from Turkey. Applied Radiation Isotopes 69, 1299–1306.

Vandenabeele, P., 2010. Raman spectroscopy. Analytical and Bioanalytical Chemistry 397, 2629–2630.

WEBMINERAL, 2011. Minerals arranged by X-Ray powder diffraction via <http://webmineral.com/MySQL/xray.php>.

Weil, J.A., 1984. A review of electron spin spectroscopy and its application to the study of paramagnetic defects in crystalline quartz. Physics and Chemistry of Minerals 10, 149–165.

Yılmaz, I.Ö., Altıner, D., Tekin, U.K., Tüysüz, O., Ocakoğlu, F., Açıkalın, S., 2010. Cenomanian–Turonian Oceanic Anoxic Event (OAE2) in the Sakarya Zone, northwestern Turkey: Sedimentological, cyclostratigraphic, and geochemical records. Cretaceous Record 31, 207–226.

Zhao, Th., Yan, X.W., Cui, J., 1994. The physical and chemical properties of synthetic and natural jadeite for jewellery. Journal of Material Sciences 29, 1514–1520.